Research Journal of Applied Sciences, Engineering and Technology 7(3): 521-526, 2014
DOI:10.19026/rjaset.7.285
ISSN: 2040-7459; e-ISSN: 2040-7467

Submitted: February 07, 2013 Accepted: March 03, 2013 Published: January 20, 2014

Research Article

Angle Estimation in Bistatic MIMO Radar System based on Unitary ESPRIT

Ebregbe David, Deng Weibo and Yang Songyan
School of Electronics and Information Engineering, Harbin Institute of Technology, Harbin 15001, China

Abstract: Angle estimation for a bistatic MIMO radar system based on Unitary Esprit techniques is proposed in this study. The algorithm exploits the dual invariance in distinct directions and centrosymmetry of the bistatic MIMO radar system to provide real valued computations and automatically paired Directions of Departures (DOD) and Directions of Arrival (DOA) estimates. Simulation results show the effectiveness of this method.

Keywords: Centrosymmetry, invariance, orthogonal signals, radar cross section, uniform linear array doppler frequency

INTRODUCTION

There has been a surge in the study of MIMO radar systems recently following successes in MIMO communications (Bekkerman and Tabrikian, 2006). Spatial diversity gain and waveform diversity are two very important advantages coming from these studies (Bencheikh *et al*., 2010; Bencheikh and Wang, 2010; Bekkerman and Tabrikian, 2006; Chen *et al*., 2010). The MIMO radar architecture is of two types. One with both the transmitter and receiver arrays or at least one of them widely spaced, is usually called statistical MIMO radar. With this configuration, the target can be viewed from different angles, achieving spatial diversity and also smoothens out RCS fluctuations often seen by phased array systems (Haimovich *et al*., 2008). The other architecture, called collocated MIMO has both the transmit and receive array antennas closely spaced for detection and direction finding purposes (Fisher *et al*., 2004; Bekkerman and Tabrikian, 2006). These can be monostatic or bistatic. In the bistatic scheme, the transmitter and receiver arrays are far apart. Hence, Directions of Departures (DOD) and Directions of Arrival (DOA) must be estimated and paired correctly. In conventional bistatic radar DOD/DOA synchronization is achieved by the transmitting beam and the receiving beam illuminating the target simultaneously. Angle estimation in bistatic MIMO radar has been researched intensely. The desire is to obtain accurate estimates of the target locations as well as improvement on algorithms to reduce computational loads in order to meet real time demands.

Duofang *et al*. (2008) applied the subspace based ESPRIT algorithm to the bistatic MIMO radar system by exploiting the dual invariance property of the transmitting and receiving arrays. This produced two rotational matrices whose eigenvalues correspond to the DODs and DOAs. But an additional pairing algorithm to match the DODs to the DOAs is required. For uniformly spaced antennas, Bencheikh and Wang (2010) developed a combination of ESPRIT and root MUSIC formulation to achieve automatic pairing of the angles thereby avoiding an exhaustive 2D MUSIC search to determine the DODs and DOAs. In all of these studies, reduction in algorithm complexity and pairing has been achieved in different ways.

The foundation, for this study is based on Lee's (1980) pioneering work on centro-hermitian matrices, in converting a complex matrix to a real matrix using a Unitary transform. Haardt and Nossek (1995, 1998) applied these transforms to the ESPRIT algorithm to develop the Unitary ESPRIT algorithm and its variants for multidimensional arrays.

In this proposal, we apply the unitary ESPRIT technique to a bistatic MIMO radar scheme and develop different selection matrices. The main idea is to use real valued computations throughout except for the final step for pairing purposes. The computational load is reduced and resolution increased.

METHODOLOGY

Signal model: Consider a narrowband bistatic MIMO radar system consisting of M and N half-wavelength spaced omnidirectional antennas for the transmitter and receiver arrays respectively. Assume both arrays are Uniform Linear Arrays (ULA) and for sake of simplicity and clarity without loss of generality, we use a simple model with P uncorrelated targets with different Doppler frequencies in the same range bin that appear in

Corresponding Author: Ebregbe David, School of Electronics and Information Engineering, Harbin Institute of Technology, Harbin 15001, China

the far field of the transmit and receive arrays. Considering also that the target Radar Cross Section (RCS) is constant during a pulse period but fluctuates from pulse to pulse, the target model is a classical swerling case II model and Doppler effects are negligible and can be ignored. The directions of the p^{th} target with respect to the transmit array normal and receive array normal are denoted by θ_p (DOD) and ϕ_p (DOA) respectively. The location of the p^{th} target is denoted by (θ_p, ϕ_p). The transmitted waveforms are M orthogonal signals with identical bandwidth and centre frequency. The coded signal of the m^{th} transmit antenna within one repetition interval is denoted by $s_m \in \mathbb{C}^{1\times L}$ where, L denotes the length of the coding sequence within one repetition interval. For a radar system that uses K periodic pulse trains to temporally sample the signal environment, the received signals of the k^{th} pulse at the receiver array through reflections of the P targets can be written as (Jin *et al*., 2009; Bencheikh *et al*., 2010; Chen *et al*., 2010):

$$\boldsymbol{X}_k = \sum_{p=1}^{P} \boldsymbol{a}_r(\phi_p)\beta_p \boldsymbol{a}_t^T(\theta_p)\begin{bmatrix} \boldsymbol{s}_1 \\ \vdots \\ \boldsymbol{s}_M \end{bmatrix} e^{j2\pi f_{dp} t_k} + \boldsymbol{W}_k \tag{1}$$

where, $X_k \in C^{MN\times L}$ and k = 1, 2, … K, β_p denotes the RCS of the p^{th} target and f_{dp} denotes the Doppler frequency of the p^{th} target. $a_r(\phi_p) = [1, e^{jr_p}, e^{j2r_p}, \dots\dots, e^{j(N-1)r_p}]^T$ and $a_t(\theta_p) = [1, e^{jt_p}, e^{j2t_p}, \dots\dots, e^{j(M-1)t_p}]^T$ are the receiver and transmitter steering vectors respectively. And $r_p = \pi \sin\phi_p$, $t_p = \pi \sin\theta_p$. $W_k \in \mathbb{C}^{NL\times K}$ is the noise matrix whose columns are Independently and Identically Distributed (IID) complex Gaussian random vectors with zero mean and covariance matrix $\sigma^2 I_N$. I_N is a NxN identity matrix. t_k denotes the slow time, k the slow time index and K the number of pulses or repetition intervals. Using the orthogonality property of the transmitted waveforms, ($s_i s_j = 0$ and $\|s_i\|^2 = 1$, $i \neq j$ = 1… M), the output of the matched filters with the m^{th} transmitted baseband signal can be expressed as:

$$\boldsymbol{Y}_m(t_k) = \sum_{p=1}^{P} \boldsymbol{a}_r(\phi_p)\beta_p \boldsymbol{a}_t^T(\theta_p)\begin{bmatrix} 0 \\ \vdots \\ 1 \\ \vdots \\ 0 \end{bmatrix} e^{j2\pi f_{dp} t_k} + \boldsymbol{V}_m(t_k) \tag{2}$$

The data matrix in Eq. (2) is usually vectorized by stacking the columns of Y_m (t_k). Let z (t_k) $\in C^{MN\times 1}$ be the output of all the received signal:

$$\boldsymbol{z}(t_k) = \left[\boldsymbol{Y}_1^T(t_k), \dots\dots\dots, \boldsymbol{Y}_M^T(t_k)\right]^T \tag{3}$$

$$\boldsymbol{z}(t_k) = \boldsymbol{A}\boldsymbol{s}(t_k) + \boldsymbol{n}(t_k) \tag{4}$$

where, $\mathrm{A} = [\mathrm{a_r}(\phi_1)\otimes \mathrm{a}_t(\theta_1), \dots\dots\dots, \mathrm{a}_r(\phi_\mathrm{p})\otimes \mathrm{a}_t(\theta_\mathrm{p})]$ is the matrix of $MN\times P$ directional vectors, $\otimes$ is the kronecker product. $\mathrm{n}(t_k) = vec(\mathrm{V}_m(t_k))$ is the additive white Gaussian noise of zero mean and covariance, $\sigma^2 I_{MN}$ after match filtering:

$$\boldsymbol{s}(t_k) = \begin{bmatrix} \beta_1 e^{j2\pi f_{d1} t_k} \\ \vdots \\ \beta_P e^{j2\pi f_{dP} t_k} \end{bmatrix}$$

Let Z denote the MN×K complex data matrix composed of K snapshots of z (t_k), $1 \le k \le K$:

$$\boldsymbol{Z} = [\boldsymbol{z}(t_1)\ \boldsymbol{z}(t_2) \cdots\cdots \boldsymbol{z}(t_K)] \tag{5}$$

$$= \boldsymbol{A}[\boldsymbol{s}(t_1)\ \boldsymbol{s}(t_2) \cdots\cdots \boldsymbol{s}(t_K)] + [\boldsymbol{n}(t_1)\ \boldsymbol{n}(t_2) \cdots\cdots \boldsymbol{n}(t_k)) \tag{6}$$

$$\boldsymbol{Z} = \boldsymbol{AS} + \boldsymbol{N} \tag{7}$$

Virtual array centrosymmetry and selection matrices: Using the forward/backward averaging property of unitary esprit, the extended data matrix becomes:

$$\boldsymbol{Z}_e = [\boldsymbol{Z}\,\Pi_{MN}\ \boldsymbol{Z}^*\,\Pi_K] \quad \in C^{MN\times 2K} \tag{8}$$

We employ the linear algebra property that the inner product between any two conjugate centrosymmetric vector is real valued, then any matrix whose rows are each conjugate centro symmetric can be applied to transform a complex valued array manifold vector into a real valued manifold. i.e., if the matrix A is centro hermitian, then Q_F^H AQ_S is a real matrix. The matrix Q is unitary, its columns are conjugate symmetric and has a sparse structure (Yilmazer *et al*., 2006). As researched by various authors based on the pioneering work of Lee (1980) the perfect matrices to accomplish this are:

$$\boldsymbol{Q}_{2F} = \tfrac{1}{2}\begin{bmatrix} \boldsymbol{I}_F & j\boldsymbol{I}_F \\ \Pi_F & -j\Pi_F \end{bmatrix} \quad \text{for even } F$$

and

$$\boldsymbol{Q}_{2F+1} = \tfrac{1}{2}\begin{bmatrix} \boldsymbol{I}_F & \boldsymbol{0} & j\boldsymbol{I}_F \\ \boldsymbol{0}^T & \sqrt{2} & \boldsymbol{0}^T \\ \Pi_F & \boldsymbol{0} & -j\Pi_F \end{bmatrix} \quad \text{for odd } F \tag{9}$$

These can be used to transform the complex valued extended data matrix to real valued matrix:

$$\boldsymbol{Z}_{real} = \boldsymbol{Q}_{MN}^H[\boldsymbol{Z}\Pi_{MN}\ \boldsymbol{Z}^*\Pi_K]\boldsymbol{Q}_{2K} \quad \in C^{MN\times 2K} \tag{10}$$

The real valued covariance matrix can be estimated using the maximum likelihood estimate:

$$\boldsymbol{R}_{Z_{real}} = \tfrac{1}{2K}\left(\boldsymbol{Z}_{real}\boldsymbol{Z}_{real}^H\right) \tag{11}$$

Eigen-decomposition of $R_{Z_{real}}$ yields a signal subspace matrix E_s composed of the P eigenvectors corresponding to the P largest eigenvalues.

Let $T_p = e^{jt_p}$ and $R_p = e^{jr_p}$, $a_r(\phi_p) = [1, R_p, R_p^2, \ldots\ldots R_p^{N-1}]^T$ and $a_t(\theta_p) = [1, T_p, T_p^2, \ldots\ldots T_p^{M-1}]^T$. Each column of A corresponds to a MN element virtual array for the p^{th} target:

$$\boldsymbol{A}_{(MN,p)} = \boldsymbol{a}_r(\phi_p) \otimes \boldsymbol{a}_t(\theta_p) \tag{12}$$

$$= [1, T_p, \ldots, T_p^{M-1}, R_p, R_pT_p, \ldots, R_pT_p^{M-1}, \ldots, R_p^{N-1}, R_p^{N-1}T_p, \ldots, R_p^{N-1}T_p^{M-1}]^T \tag{13}$$

Exploring, the structure of the MN element virtual array manifold, $A_{(MN,\,p)}$ of the p^{th} target, the two pairs of selection matrices for each of the transmit and receive arrays must be choosen to be centrosymmetric with respect to one another from the array manifold.

The maximum overlap sub-arrays consisting of the first and last M-1 elements of the transmit array steering vectors, $\alpha_t(\theta_p)$ in the complete MN virtual array occurs N times. The selection matrices are J_1 and J_2 both M-1×M-1 matrices occurring N times:

$$\boldsymbol{J}_1 = \boldsymbol{I}_{N\times N} \otimes \begin{bmatrix} \boldsymbol{I}_{(M-1)\times(M-1)} & \boldsymbol{0}_{(M-1)\times 1} \end{bmatrix} \tag{14}$$

$$\boldsymbol{J}_2 = \boldsymbol{I}_{N\times N} \otimes \begin{bmatrix} \boldsymbol{0}_{(M-1)\times 1} & \boldsymbol{I}_{(M-1)\times(M-1)} \end{bmatrix} \tag{15}$$

$$\boldsymbol{J}_2 = \Pi_{(M-1)N}\, \boldsymbol{J}_1 \Pi_{MN} \tag{16}$$

The shift invariance property for the transmit array from the columns of A can be expressed as:

$$(\boldsymbol{J}_1)^{Blk} \boldsymbol{A} = (\boldsymbol{J}_2)^{Blk} \boldsymbol{A\Phi}_t \tag{17}$$

where, $(\cdot)^{Blk} = \text{blkdiag}(\cdot)$ denotes block diagonal matrix, and $\Phi_t = diag\{e^{jt_p}\}_{p=1}^{P}$. The elements of the receive array steering vectors, $a_r(\phi_p)$ are stretched across the MN virtual array, i.e., each element occurs M times in the MN virtual array. Therefore the maximum overlap sub-arrays of the receive steering vectors consists of the first and last M (N-1) of the MN virtual array elements. The selection matrices for the receive array are as follows:

$$\boldsymbol{J}_3 = \begin{bmatrix} \boldsymbol{I}_{M(N-1)\times M(N-1)} & \boldsymbol{0}_{M(N-1)\times M} \end{bmatrix} \tag{18}$$

$$\boldsymbol{J}_4 = \begin{bmatrix} \boldsymbol{0}_{M(N-1)\times M} & \boldsymbol{I}_{M(N-1)\times M(N-1)} \end{bmatrix} \tag{19}$$

And also posses centrosymmetry with respect to each other:

$$\boldsymbol{J}_4 = \Pi_{M(N=1)} \boldsymbol{J}_3 \Pi_{MN} \tag{20}$$

$$\boldsymbol{J}_3 \boldsymbol{A} = \boldsymbol{J}_4 \boldsymbol{A\Phi}_r \tag{21}$$

where,

$$\Phi_r = diag\left\{e^{jr_p}\right\}_{p=1}^{P}$$

Joint angle estimation using unitary esprit: The Unitary transformed virtual array steering matrix is obtained as (Haardt and Nossek, 1995; Zoltowski *et al*., 1996):

$$\boldsymbol{G} = \boldsymbol{Q}_{MN}^{H} \boldsymbol{A} \tag{22}$$

The transformed selection matrices and invariance equations can be obtained by substituting Eq. (22) into (17) and (21):

$$(\boldsymbol{J}_1)^{Blk} \boldsymbol{Q}_{MN} \boldsymbol{Q}_{MN}^{H} \boldsymbol{A} = \boldsymbol{\Phi}_t (\boldsymbol{J}_2)^{Blk} \boldsymbol{Q}_{MN} \boldsymbol{Q}_{MN}^{H} \boldsymbol{A} \tag{23}$$

$$(\boldsymbol{J}_1)^{Blk} \boldsymbol{Q}_{MN} \boldsymbol{G} = \boldsymbol{\Phi}_t (\boldsymbol{J}_2)^{Blk} \boldsymbol{Q}_{MN} \boldsymbol{G} \tag{24}$$

Pre-multiplying both sides by $Q_{(M-1)N}^{H}$ gives the invariance equation for the transmit array as:

$$\boldsymbol{Q}_{(M-1)N}^{H} (\boldsymbol{J}_1)^{Blk} \boldsymbol{Q}_{MN} \boldsymbol{G} = \boldsymbol{\Phi}_t \boldsymbol{Q}_{(M-1)N}^{H} (\boldsymbol{J}_2)^{Blk} \boldsymbol{Q}_{MN} \boldsymbol{G} \tag{25}$$

Making use of Eq. (21):

$$\Pi_n \boldsymbol{Q}_n = \boldsymbol{Q}_n^* \text{ and } \Pi_n \Pi_n = \boldsymbol{I}_n$$

$$\begin{aligned} \boldsymbol{Q}_{(M-1)N}^{H} (\boldsymbol{J}_2)^{Blk} \boldsymbol{Q}_{MN} &= \boldsymbol{Q}_{(M-1)N}^{H} \Pi_{(M-1)N} \Pi_{(M-1)N} (\boldsymbol{J}_2)^{Blk} \Pi_{MN} \Pi_{MN} \boldsymbol{Q}_{MN} \\ &= \boldsymbol{Q}_{(M-1)N}^{T} (\boldsymbol{J}_1)^{Blk} \boldsymbol{Q}_{MN}^{*} \\ &= (\boldsymbol{Q}_{(M-1)N}^{H} (\boldsymbol{J}_1)^{Blk} \boldsymbol{Q}_{MN})^{*} \end{aligned} \tag{26}$$

$$\boldsymbol{K}_1 = \text{Re}\left\{(\boldsymbol{Q}_{(M-1)N}^{H} (\boldsymbol{J}_2)^{Blk} \boldsymbol{Q}_{MN})\right\} \tag{27}$$

$$\boldsymbol{K}_2 = \text{Im}\left\{(\boldsymbol{Q}_{(M-1)N}^{H} (\boldsymbol{J}_2)^{Blk} \boldsymbol{Q}_{MN})\right\} \tag{28}$$

Substituting in Eq. (25), we have:

$$\left(\boldsymbol{Q}_{(M-1)N}^{H} (\boldsymbol{J}_2)^{Blk} \boldsymbol{Q}_{MN}\right)^{*} \boldsymbol{G} = \boldsymbol{\Phi}_t \left(\boldsymbol{Q}_{(M-1)N}^{H} (\boldsymbol{J}_2)^{Blk} \boldsymbol{Q}_{MN}\right) \boldsymbol{G} \tag{29}$$

$$\boldsymbol{\Phi}_t \left(\boldsymbol{K}_1 - j\boldsymbol{K}_2\right) \boldsymbol{G} = \left(\boldsymbol{K}_1 + j\boldsymbol{K}_2\right) \boldsymbol{G} \tag{30}$$

Multiplying both sides by $e^{-jt_{p/2}}$ gives:

$$e^{-jt_p/2} \boldsymbol{\Phi}_t \left(\boldsymbol{K}_1 - j\boldsymbol{K}_2\right) \boldsymbol{G} = e^{-jt_p/2} \boldsymbol{I}_P \left(\boldsymbol{K}_1 + j\boldsymbol{K}_2\right) \boldsymbol{G} \tag{31}$$

Note that $\Phi_t = \text{diag}\ \{e^{jt_p}\}_{p=1}^{P}$ and rearranging we have:

Table 1: Target locations, RCSs and Doppler frequencies

Targets	1	2	3	4	5	6	7	8
DOD (θ)	-20	-50	-10	-40	60	30	40	20
DOA (ϕ)	-40	-20	10	40	0	50	30	-25
β	1	1	1	1	1	1	1	1
f_d (Hz)	1000	1500	2000	2500	3000	3500	4000	4500

$$\left(e^{jt_p/2}\boldsymbol{I}_P - e^{-jt_p/2}\boldsymbol{I}_P\right)\boldsymbol{K}_1 G = j\left(e^{jt_p/2}\boldsymbol{I}_P - e^{-jt_p/2}\boldsymbol{I}_P\right)\boldsymbol{K}_2 G \quad (32)$$

Making use of the tangent identity:

$$\tan\left(t/2\right) = \frac{e^{jt/2} - e^{-jt/2}}{j\left(e^{jt/2} + e^{-jt/2}\right)} \quad (33)$$

$$diag\left\{\tan\left(t_p/2\right)\right\}_{p=1}^{P} \boldsymbol{K}_1\boldsymbol{G} = \boldsymbol{K}_2\boldsymbol{G} \quad (34)$$

We have the following transformed real valued invariance equation for the transmit array:

$$\boldsymbol{K}_1\boldsymbol{G}\boldsymbol{\Omega}_t = \boldsymbol{K}_2\boldsymbol{G} \quad (35)$$

where,

$$\Omega_t = diag\{\tan(t_p/2)\}_{p=1}^{P}$$

The MN×P real valued matrix of signal eigenvectors E_s spans the same P dimensional subspace as the 2 MN×P real valued steering matrix G. Therefore there exists a nonsingular matrix H of size P×P such that $E_s = GH$.

Substituting this in Eq. (35) yields the transformed invariance equation which computes the DODs:

$$\boldsymbol{K}_1\boldsymbol{E}_s\boldsymbol{\Psi}_t = \boldsymbol{K}_2\boldsymbol{E}_s \quad (36)$$

where, $\Psi_t = H\Omega_t H^{-1}$. Following the same procedure, the transformed selection matrices and invariance equations to compute the DOAs for the receiver array are obtained as:

$$\boldsymbol{K}_3 = \mathrm{Re}\left\{(\boldsymbol{Q}^H_{M(N-1)}\boldsymbol{J}_4\,\boldsymbol{Q}_{MN})\right\} \quad (37)$$

$$\boldsymbol{K}_4 = \mathrm{Im}\left\{(\boldsymbol{Q}^H_{M(N-1)}\boldsymbol{J}_4\,\boldsymbol{Q}_{MN})\right\} \quad (38)$$

$$\boldsymbol{K}_3\boldsymbol{G}\boldsymbol{\Omega}_r = \boldsymbol{K}_4\boldsymbol{G} \quad (39)$$

where,

$$\boldsymbol{\Omega}_r = diag\left\{\tan\left(r_p/2\right)\right\}_{p=1}^{P}$$

And the invariance equation to compute the DOAs is obtained as:

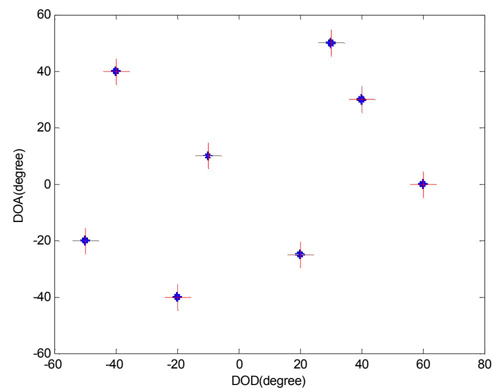

Fig. 1: Joint angle estimation for the proposed algorithm for 8 targets over 500 monte carlo trials with SNR = 10 dB

$$\boldsymbol{K}_3\boldsymbol{E}_s\boldsymbol{\Psi}_r = \boldsymbol{K}_4\boldsymbol{E}_s \quad (40)$$

where, $\Psi_r = H\Omega_r H^{-1}$.

Since both ψ_t and ψ_r share the same transform matrix H and are also real valued matrices, automatically paired estimates of DODs and DOAs $\{t_p, r_p\}$, p = 1…p can be obtained from the real and imaginary parts of the eigenvalues obtained by the eigen-decomposition of the complex valued matrix:

$$\boldsymbol{\Psi}_t + j\boldsymbol{\Psi}_r = \boldsymbol{H}\left(\boldsymbol{\Omega}_t + j\boldsymbol{\Omega}_r\right)\boldsymbol{H}^{-1} \quad (41)$$

where, $\Omega_t + j\Omega_r = \mathrm{diag}\ \{\lambda_p\}^P_{p=1}$, are the eigenvalues. The DODs and DOAs are obtained as:

$$\hat{\theta}_p = \arcsin\left\{2\arctan\left(\mathrm{Re}\left\{\lambda_p\right\}\right)\right\} \quad 1 \le p \le P \quad (42)$$

$$\hat{\phi}_p = \arcsin\left\{2\arctan\left(\mathrm{Im}\left\{\lambda_p\right\}\right)\right\} \quad 1 \le p \le P \quad (43)$$

SIMULATION RESULTS AND DISCUSSION

In this section, we perform simulations to evaluate the performances of the algorithm proposed in this study. First, we consider a Uniform Linear Array (ULA) of 3 antennas at the transmitter and 4 antennas at the receiver, both of which have half wavelength spacing between its antennas. There are 8 targets with locations, RCSs and Doppler frequencies as shown in Table 1. The pulse repetition frequency is 10 kHz. The operating frequency is 30 GHz and the pulse width is 10 µs. The SNR = 10 dB. We observed 256 snapshots of the received signal corrupted by a zero mean spatially white noise with variance 1. For purpose of statistical repeatability, we made 500 monte carlo trials.

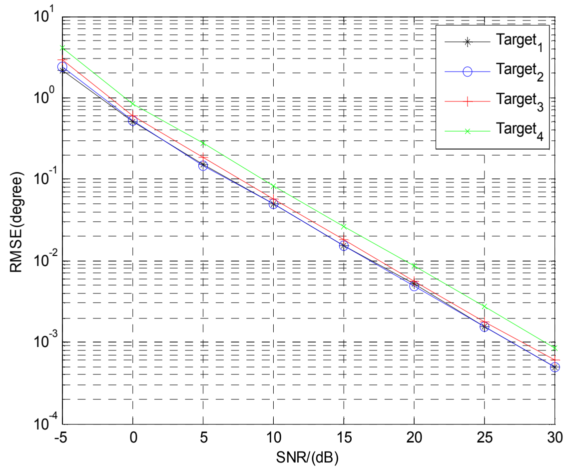

Fig. 2: RMSE of estimation of P = 4 targets versus SNR with M = 8, N = 6, K = 256 for 200 monte carlo trials

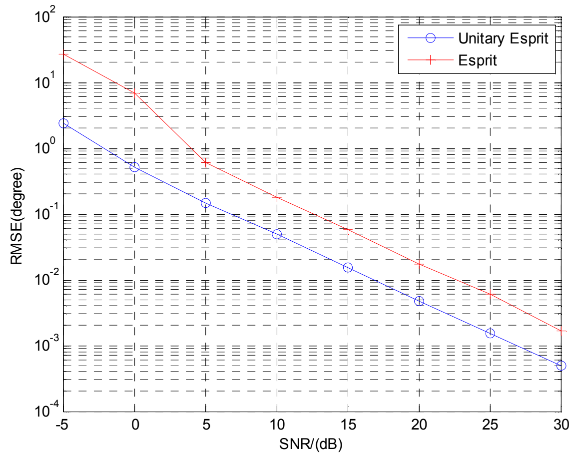

Fig. 3: RMSE of estimation versus SNR for M = 8, N = 6 and K = 256 samples for 200 monte carlo trials

In Fig. 1, the scatter plot shows the targets are localized and automatically paired correctly.

In this part, we evaluate the performance of the algorithm with 4 targets from angles $(\theta_1, \phi_1) = (10°, 20°)$, $(\theta_2, \phi_2) = (-8°, 30°)$, $(\theta_3, \phi_3) = (0°, 45°)$, $(\theta_4, \phi_4) = (50°, 60°)$, with reflection coefficients $\beta_1 = \beta_2 = \beta_3 = \beta_4 = 1$ and Doppler frequencies $f_{d1} = 1000$ Hz, $f_{d2} = 1500$ Hz, $f_{d3} = 2500$ Hz and $f_{d4} = 3000$ Hz. We use the Root Mean Square Error (RMSE) performance criterion. The RMSE of the p^{th} target angle estimation is defined as:

$$\text{RMSE}_p = \sqrt{\frac{1}{L}\sum_{l=1}^{L}\left(\hat{\theta}_{pl} - \theta_p\right)^2 + \left(\hat{\phi}_{pl} - \phi_p\right)^2}$$

where,

L : The monte carlo trial

$\hat{\theta}_{pl}$ and $\hat{\phi}_{pl}$: The estimates at the l^{th} iteration

θ_p & ϕ_p : True values

The number of samples is K = 256 and SNRs from -5 to 30 dB. We consider a bistatic MIMO radar constituted of M = 8 transmitters and N = 6 receivers. We retain the same antenna spacing as the first simulation. The results are obtained using 200 monte carlo simulations. Figure 2 shows the RMSE versus SNR for the 4 targets. The estimation errors are quite negligible.

The next simulation compares the RMSE of target angle estimation of the proposed algorithm to that for esprit algorithm in a bistatic MIMO radar system. The parameters and simulation conditions are the same as the previous simulation. Figure 3 gives a comparison of the RMSE for Unitary esprit and the RMSE for esprit versus different SNRs for one target. The RMSEs for the other targets are similar. From Fig. 3, shows that for as low as -5 dB SNR, the proposed algorithm yields excellent estimates with low errors. Furthermore, this estimator clearly performs better for both low and high SNRs, than the esprit algorithm.

CONCLUSION

In this study, the unitary ESPRIT technique is applied to a bistatic MIMO radar system to estimate target angles by exploiting the dual invariance structure of the bistatic MIMO radar system. The simulation results show that the proposed algorithm provides better performances in angle estimation than the ESPRIT algorithm. The number of targets that can be detected is increased and there is a lower computational complexity as the algorithm uses only real valued computations.

ACKNOWLEDGMENT

This study was supported by the National Natural Science Foundation of China under Grant No. 61171182.

REFERENCES

Bekkerman, I. and J. Tabrikian, 2006. Target detection and localization using MIMO radars and sonars. IEEE T. Signal Process., 54(10): 3873-3883.

Bencheikh, M.L. and Y. Wang, 2010. Joint DOD-DOA estimation using combined ESPRIT-MUSIC approach in MIMO radar. IET Electr. Lett., 46(15): 1081-1083.

Bencheikh, M.L., Y. Wang and H. He, 2010. Polynomial root finding technique for joint DOA DOD estimation in bistatic MIMO radar. Signal Process., 90(9): 2723-2730.

Chen, J.L., H. Gu and W.M. Su, 2010. A new method for joint DOD and DOA estimation in bistatic MIMO radar. Signal Process., 90: 714-718.

Duofang, C., C. Baixiao and Q. Guodong, 2008. Angle estimation using ESPRIT in MIMO radar. IEEE Electr. Lett., 44(12): 770-771.

Fisher, E., A. Haimovich, R.S., Blum, D. Chizhik, L.J. Jr. Cimini and R. Valenzuela, 2004. MIMO radar: An idea whose time has come. Proceeding of the IEEE Radar Conference. Philadelphia, PA, USA, pp: 71-78.

Haardt, M. and J.A. Nossek, 1995. Unitary ESPRIT: How to obtain increased estimation accuracy with a reduced computational burden. IEEE T. Signal Process., 43: 1232-1242.

Haardt, M. and J.A. Nossek, 1998. Simultaneous Schur decomposition of several non- symmetric matrices to achieve automatic pairing in multidimensional harmonic retrieval problems. IEEE T. Signal Process., 46: 161-169.

Haimovich, A.M., R. Blum and L. Cimini, 2008. MIMO radar with widely separated antennas. IEEE Signal Process. Mag., 25(1): 116-129.

Jin, M., G. Liao and J. Li, 2009. Joint DOD and DOA estimation for bistatic MIMO radar. Signal Process., 89: 244-251.

Lee, A., 1980. Centrohermitian and skew-centrohermitian matrices. Lin. Algebra Appl., 29: 205-210.

Yilmazer, N., J. Koh and T.K. Sarkar, 2006. Utilization of a unitary transform for efficient computation in the matrix pencil method to find the direction of arrival. IEEE T. Antenn. Propag., 54(1): 175-181.

Zoltowski, M.D., M. Haardt and C.P. Mathews, 1996. Closed-form 2-D angle estimation with rectangular arrays in element space or beam space via unitary ESPRIT. IEEE T. Signal Proces., 44(2): 316-328.